analytical chemistry

Article

Cite This: *Anal. Chem.* 2019, 91, 912–918

pubs.acs.org/ac

# Surface Acoustic Wave Nebulization with Atmospheric-Pressure Chemical Ionization for Enhanced Ion Signal

Linxia Song,[†] Yi You,[‡] and Theresa Evans-Nguyen*[,†]

[†]University of South Florida, Tampa, Florida 33620, United States

[‡]Federal Institute for Materials Research and Testing (BAM), 12489 Berlin, Germany

Supporting Information

**ABSTRACT:** Many ambient desorption/ionization mass spectrometry (ADI-MS) techniques rely critically on thermal desorption. Meanwhile, the analyte classes that are successfully studied by any particular ADI-MS methods are strongly dependent on the type of ionization source. Generally, spray-based ionization sources favor polar analytes, whereas plasma-based sources can be used for more hydrophobic analytes and are more suitable for molecules with small molar masses. In the present work, classic atmospheric-pressure chemical ionization (APCI) is used. To provide improved desorption performance for APCI, a surface acoustic wave nebulization (SAWN) device was implemented to convert liquid analytes into fine airborne particles. Compared to conventional SAWN that is used solely as an ionization source for liquid samples, the coupling of SAWN and APCI significantly improves ion signal by up to 4 orders of magnitude, reaching comparable ion abundances to those of electrospray ionization (ESI). Additionally, this coupling also extends the applicable mass range of an APCI source, conventionally known for the ionization of small molecules <500 Da. Herein, we discuss cursory evidence of this applicability to a variety of analytes including both polar and nonpolar small molecules and novel peptides that mimic biomolecules upward of 1000 Da. Observed species are similar to ESI-derived ions including doubly charged analyte ions despite presumably different charging mechanisms. SAWN–APCI coupling may thus involve more nuanced ionization pathways in comparison to other ADI approaches.

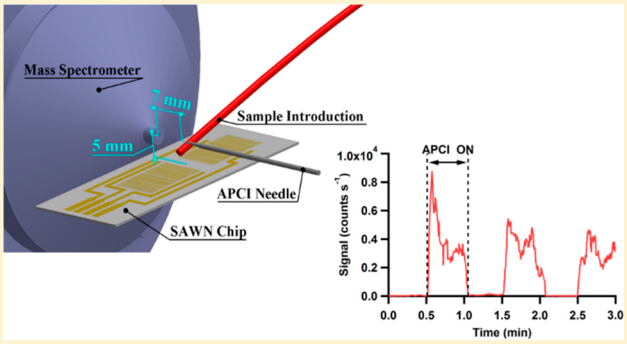


Downloaded via UNIV OF SOUTH FLORIDA on April 21, 2021 at 18:05:29 (UTC).
See https://pubs.acs.org/sharingguidelines for options on how to legitimately share published articles.

Over the past two decades, ambient desorption/ionization techniques have drawn significant attention in mass spectrometric instrumentation development,[1,2] spawning various commercial products. In 2004, Cooks et al.[3] introduced the term ambient desorption/ionization mass spectrometry (ADI-MS), which described methods that provide direct desorption/ionization of analytes with minimal sample preparation in an ambient environment. Spray-based approaches including desorption electrospray ionization (DESI) use electrically charged droplets to desorb/ionize analyte of interest from surfaces.[3] Plasma-based approaches, including the commercially available ones such as direct analysis in real time (DART), typically achieve thermal desorption of analytes and subsequent ionization through ion–molecular interactions.[4] However, the types of compounds that are suitable to be analyzed by each individual method can be limited.[1,5] For instance, spray-based techniques may ionize molecules across a wide range of mass-to-charge ratios ($m/z$) but are commonly used for moderately to highly polar analytes.[5] In contrast, methods employing electrical plasmas (e.g., flowing atmospheric-pressure afterglow (FAPA) and DART) are capable of ionizing polar and nonpolar analytes but primarily for those with low molecular masses.[1,6,7] Thus far, developments of universal ionization methods, which do not depend on the polarity or the molecular weight of the analyte, still remain challenging for ADI-MS.

In ADI-MS, efficient conversion of nonvolatiles from condensed to gas phase can be complicated for ionization sources with intimately coupled desorption mechanisms. Commonly, a peripheral heater is implemented to promote thermal desorption,[8] but competing processes of thermal decomposition can severely limit the mass range for intact molecular ions.[6,9] Alternative desorption methods such as drop-on-demand[10] and laser ablation[11] prove to be especially useful for analytes with very low vapor pressures.[12] Such options helped to avoid high desorption temperatures, which facilitate decomposition.

A novel technology termed surface acoustic wave nebulization (SAWN) had been demonstrated for liquid sample preparation from microfluidics.[13,14] Specifically for desorption/atomization and as a self-contained ionization source in mass spectrometry, SAWN was pioneered by the laboratories of Goodlett[15−19] and others.[20,21] Briefly, the surface acoustic wave is generated through the electrodes embedded onto a

**Received:** August 28, 2018
**Accepted:** November 27, 2018
**Published:** November 27, 2018


© 2018 American Chemical Society

DOI: 10.1021/acs.analchem.8b03927
*Anal. Chem.* 2019, 91, 912–918

dielectric chip, on which a liquid sample droplet is maintained. The acoustic energy transferred to the droplet overcomes its surface tension leading to atomization.[13,20] During the atomization, fine particles are produced, where a small fraction of them are charged speculatively because of microscopic fluctuations in the bulk liquid.[22,23] Such a nebulization/ionization process has been applied to polar and nonpolar analytes, such as peptides and lipids.[24,25] Although SAWN is capable of generating ESI-like mass spectra, the ion signal from a SAWN is commonly 2−3 orders of magnitude lower than that with an ESI,[25] limiting SAWN's applications. However, the simple geometry of SAWN devices allows potentially attractive combinations with other ionization techniques to potentially improve overall ionization efficiency.

Therefore, in the present work, we sought to couple a SAWN device with an APCI source to enhance the ionization efficiency compared to conventional SAWN. Under atmospheric conditions, a corona discharge is formed at the tip of an APCI needle when a high voltage is applied.[26] Reagent ions (e.g., $(H_2O)_n{\cdot}H^+$, $O_2^+$, $NO_3^-$, etc.), which are produced by the corona discharge in air,[27] ionize analytes through various reaction schemes. For instance, protonated water clusters promote ionization by proton-transfer reactions,[28] which result in mass spectra containing the pseudomolecular ion in protonated form, $MH^+$. Meanwhile, $O_2^+$ is capable of ionizing nonpolar analyte through charge-transfer reactions, which would result in the formation of molecular ions, $M^{+\bullet}$.[29] In addition, free electrons in the very-near proximity of the plasma region also allow molecular ionization through processes such as electron capture.[30,31] Therefore, we implement SAWN primarily as a desorption process to softly convert liquid samples to airborne bare molecules (vapor) and fine particles (i.e., aerosols). Further addition of an APCI needle serves the distinct role of an ionization source, where the ionizations of analyte vapor and analyte-containing aerosols are promoted. Herein, we report that the coupling of APCI with SAWN improves the ionization efficiency for both polar and nonpolar molecules, such as caffeine and perylene, as well as species of high molar masses such as peptides. Compared to SAWN alone, typical ion signal was enhanced up to 4 orders of magnitude, leading to comparable ion signals from an ESI source.

## EXPERIMENTAL SECTION

**Chemicals.** Optima LC/MS grade solvents, including methanol (L454-4), water (W7-4), and formic acid (A117-50) were purchased from Fisher Scientific (Fair Lawn, NJ). A 1 mg/L standard caffeine solution was purchased from Acros (Geel, Belgium), which was prepared as concentrations of 1 and 10 μg/mL in 50:50 (v:v) methano/water with 0.5% formic acid. Perylene was purchased from Sigma-Aldrich (St. Louis, MO) and prepared as a 10 μg/mL solution in methanol. A standard peptide and protein sample kit (MSCAL1-1KT) was purchased from Sigma-Aldrich (St. Louis, MO). Other novel peptides (cf. Figure S1) $C_{35}H_{62}N_6O$ ($C_{12}$−Lys−Lys′−$NH_2$, termed Peptide-1) and $C_{56}H_{95}N_9O_6$ ($C_{16}$−Lys−Lys′−Lys′−$NH_2$, termed Peptide-2) were kindly provided by Dr. Jianfeng Cai's research laboratory (Department of Chemistry, University of South Florida, Tampa, FL). All peptides were solubilized using methanol/water 50:50 (v:v) with 0.5% formic acid solution. The angiotensin II was prepared in solutions of five concentrations, i.e., 1, 2, 5, 10, and 20 μg/mL; other peptides were prepared as 10 μg/mL.

**SAWN Device.** The SAWN power supply (SAWN controller V2.0) and SAWN standing wave chips V2.0 were purchased from Deurion LLC (Seattle, WA). The fabrication and operation of SAWN chips have been reported in previous publications.[18,19,24,25,32] The SAWN used in this study operates at 9.56 MHz. The droplets were introduced onto the SAWN chip continuously via an ∼70 cm peek tubing (inner diameter = 50 μm), which was placed above the geometric center of the SAWN chip surface. The analyte-containing solutions were continuously supplied to the SAWN chip with a syringe pump at a flow rate of 8 μL/min.

**APCI Source.** In this study, three APCI and APCI-like sources with different geometries were used: (i) The primary APCI source described in this work was fashioned from a commercial APCI needle from Thermo Fisher (Fair Lawn, NJ), where the needle was connected to a high-voltage power supply (PS350, Stanford Research System, Sunnyvale, CA) in series with a 6 kΩ current-limiting resistor. In addition, a homemade inductor of ∼60 μH was connected in series with the resistor and needle to prevent sudden change of current, namely avoiding arcing. The typical voltage applied to the corona needle was +3 kV at ca. 1 μA. (ii) The APCI needle was replaced by one with modified shape but in the same geometry as described above. Instead of a conventional needle tip, a round tungsten bar (Φ = 2 mm) with a polished spherical tip was used with the same setup. (iii) Differently, the other APCI source was used to investigate the ionization mechanism. Specifically, the corona discharge was confined in a quartz discharge chamber with flowing nitrogen (cf. Figure S2). Thus, direct exposure of analytes to the discharge was avoided. The ion exit is a polished brass ring (Φ = 6 mm) serving as the ground electrode. The sharpened tungsten electrode of 2 mm diameter was connected to the same power supply through a current-limiting resistor of 5 MΩ. The voltage and current applied to the tungsten electrode were +3 kV and ca. 7 μA, respectively. The gas flow rate was controlled by a valved flowmeter (SK-32461−50, Cole Parmer, Vernon Hills, IL). The flow rate was 0.5 L/min. In addition, the power supply was operated in voltage-limiting mode for all APCI sources.

**Mass Spectrometer.** All mass spectra were recorded with a commercial linear ion-trap mass spectrometer (LTQ XL, Thermo Scientific, San Jose, CA) in positive ion mode. The temperature of the ion-transfer tube was maintained at 255 °C unless otherwise specified. The capillary voltage of LTQ was maintained at 35 V. The ion-injection and acquisition parameters included a maximum injection time of 200 ms and three microscans, respectively. For caffeine, the mass range was set to $m/z$ 50−350, while for perylene, the mass range was set to $m/z$ 50−500. For peptides, the mass ranges were set based on the molecular weights of the analytes, which were 200−700 for Peptide-1, 200−1000 for Peptide-2, and 200−1200 for angiotensin II. The instrument was tuned by ESI for each analyte *m/z prior to each SAWN−APCI experiment*.

**Geometry.** The APCI needle was visually aligned coaxially with the inlet capillary of the mass spectrometer to simplify component geometry. The distance between the APCI needle and the mass spectrometer inlet was set at 7 mm. Sample introduction in the form of the nebulization plume was positioned roughly equidistant between the inlet capillary and the APCI needle (cf. Figure 1). Vertically, the chip was 5 mm below the inlet capillary, allowing optimal interactions between the upward bound analyte-containing aerosols with the APCI source. To achieve a continuous plume, the peek tubing was


DOI: 10.1021/acs.analchem.8b03927
Anal. Chem. 2019, 91, 912−918

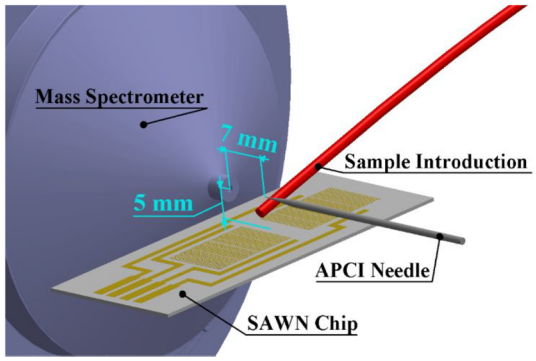


**Figure 1.** Schematic of SAWN–APCI coupling. The SAWN chip was placed 5 mm below the inlet capillary. The distance between the APCI needle and capillary inlet was 7 mm.

placed above the SAWN chip with minimal contact. To compare SAWN and SAWN–APCI, all experimental conditions (e.g., solution compositions, configurations of the mass spectrometer, and positioning) were kept the same.

## RESULTS AND DISCUSSION

**Assessing Inlet-Temperature Dependency.** In previous reports, the ion signal obtained through SAWN has been known to exhibit large variations over time compared to ESI.[24] Before coupling with APCI, the operating parameters of the SAWN device were optimized including contact angles, distance to the inlet capillary, flow rate, solvent composition, and inlet-capillary temperature. Because we ultimately seek out both neutrals and charged droplets produced by the SAWN, the effects of ion signal depending on the temperature of the ion inlet-capillary in particular was carefully investigated.[33,34] Specifically, a single droplet of caffeine solution (10 $\mu$g/mL) was placed onto the SAWN chip for each individual temperature measurement. In this manner, the ion signal of caffeine with respect to the inlet-capillary temperature was recorded and is presented in Figure 2. Between 150 to 300 °C,

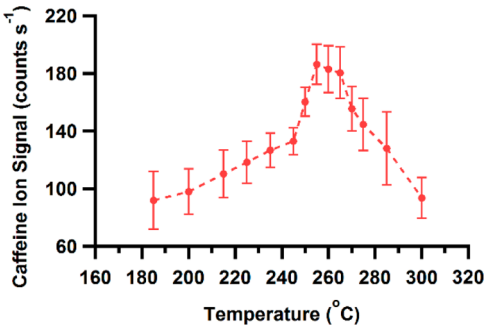


**Figure 2.** Temperature dependence of caffeine ion signal at $m/z$ 195.1. Each point on this figure was extracted with an $m/z$ range from 194.6 to 195.6. The signal variation was later assessed through the extracted ion chronogram corresponding to this range.

we determined an optimal inlet-capillary temperature at 255 °C, at which the maximal protonated ion signal for caffeine was found. Presumably, with increasing temperature up to ~250 °C, passive heating facilitates particle desolvation. Charged droplets hence evaporate down to ions, even if they are not preformed in solution. Meanwhile, at temperatures above ~250 °C, the ion signal decreases, which could be attributed to thermal decomposition and/or collision-induced charge losses.

**Enhancements in Ion Signals for Polar and Nonpolar Analytes.** In Figure 3, subsequent comparisons between SAWN alone and SAWN–APCI were performed with a caffeine solution of 1 $\mu$g/mL with a continuous liquid feeding at a flow rate of 8 $\mu$L/min. While manually engaging and disengaging the high voltage that was applied onto the APCI needle, significant signal enhancement of protonated caffeine ($m/z$ 195.1) was observed (cf. Figure 3a). With APCI activated, the caffeine signal suggests that by leveraging the abundant neutrals, overall ionization efficiency was increased by 3 orders of magnitude. In a control experiment, a droplet of the same caffeine sample was directly exposed to the APCI needle without activating the SAWN; caffeine was not detected, as expected. Relying on surface evaporation alone, caffeine's low vapor pressure of $1.2 \times 10^{-9}$ bar[35] limits its detection with the APCI needle near the bulk solution. Thus, the SAWN clearly contributed to the desorption process while coupling with APCI.

Upon closer inspection of the mass spectra, for SAWN alone (cf. Figure 3b), the protonated molecular ion is barely discernible at this concentration. Notably, the base peak ($m/z$ 216.8) is likely the sodium adduct of caffeine. By contrast, the mass spectrum recorded with the SAWN–APCI was found highly similar to that with an ESI source (cf. Figure S4a). Specifically, no sodium adduct was detected with the conventional ESI source. In Figure 3c, the SAWN–APCI clearly favors the formation of the protonated caffeine, where the base peak within the mass spectrum corresponds to $MH^+$ at $m/z$ 195.1. Notably, the sodium adduct is not observed with APCI. In this example, we calculate the signal-to-noise ratio for this same sample to go from ~220 to ~1730 for the base peak in each spectrum by implementing APCI.

In addition to polar analytes, APCI allows the ionization of nonpolar species. Thus, the SAWN–APCI approach was tested with a compound of low polarity. Molecular ions of perylene, a polycyclic aromatic hydrocarbon, were produced and detected from solution using SAWN alone as shown in Figure 4a. Unlike caffeine, for which protonated ions were the major species, the mass spectrum of perylene with SAWN was dominated by singly charged perylene $M^{+\bullet}$ at $m/z$ 252.0. The signal is sufficient to also exhibit the expected $^{13}C$ isotopic peak at $m/z$ 253.0 (Figure S5). For the mass spectrum obtained with SAWN–APCI, the $M^{+\bullet}$ was below background level, while $MH^+$ ($m/z$ 253.1) was clearly observed. Instead of a charge-transfer mechanism, in which $M^{+\bullet}$ is commonly produced, the ionization regime was likely dominated by processes such as proton transfer to produce the $MH^+$.[36]

**Toward Applications: SAWN–APCI for Large Molecules.** To investigate the enhancement effect on molecules with larger mass, we used peptides as model samples to demonstrate the capabilities of the SAWN–APCI approach. In terms of peptide and protein analysis through SAWN-MS,[18] it has been shown that biomolecules, such as proteins, are not denatured by the SAWN method because of the high acoustic frequency, which prevents cavitation and sheer degradation.[13] However, as a result of the low ionization efficiency of SAWN itself, the addition of an ion funnel was needed to compensate for the overall poor sensitivity.[18] Here, SAWN–APCI was implemented to analyze peptide samples without an ion funnel. The sample of angiotensin II (monoisotopic mass of 1046.2 g mol$^{-1}$) was analyzed to assess the SAWN–APCI ionization


DOI: 10.1021/acs.analchem.8b03927
Anal. Chem. 2019, 91, 912–918

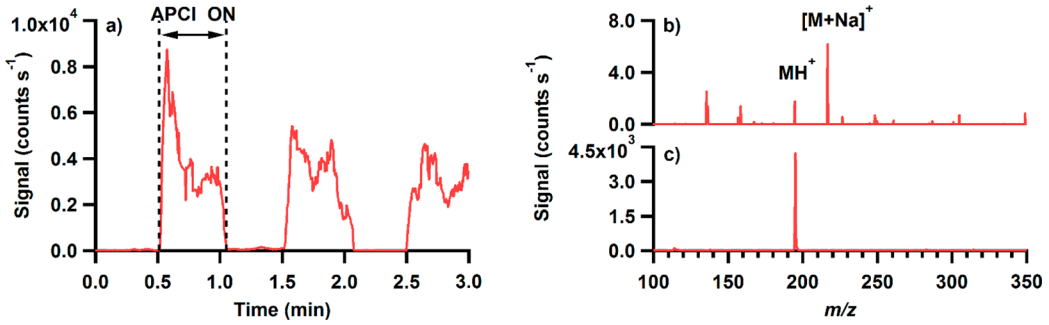


**Figure 3.** Ion chronograms and time-averaged mass spectra of caffeine. (a) Signal response of caffeine ($m/z$ 195.1) to APCI activation (extracted ion chromatogram). SAWN was continuously applied, while APCI was manually switched on and off. Note that the chronogram is smoothed. The raw ion chronogram can be found in Figure S3. (b) Time-averaged mass spectrum of caffeine with (b) APCI "off" and (c) with APCI "on".

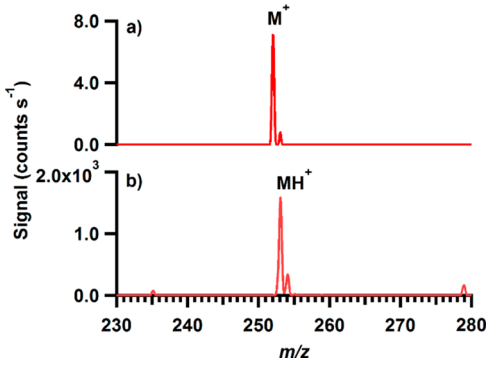


**Figure 4.** Perylene mass spectra (a) with APCI off and (b) with APCI on.

approach. The mass spectrum of angiotensin II (cf. Figure 5) from SAWN and SAWN−APCI contained a base peak

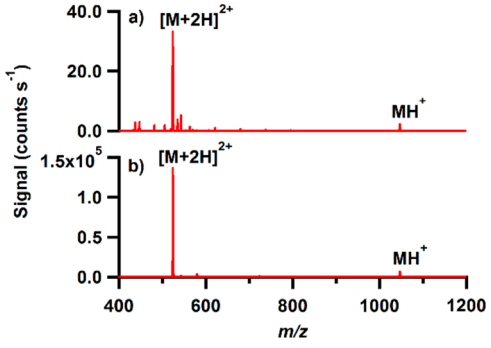


**Figure 5.** Mass spectra of angiotensin II with (a) APCI off and (b) APCI on with 10.0 $\mu$g/mL solution.

corresponding to $[M + 2H]^{2+}$. Notably, for peptide analyses, APCI produces singly charged analyte ions with low ionization efficiency;[37] it is not known to produce any multiply charged analyte ions.[38] The APCI activation led to the ion-signal enhancement for both $[M + 2H]^{2+}$ and $MH^+$ by 4 orders of magnitude compared to SAWN alone. In addition, the ion signal of doubly charged angiotensin II at $m/z$ 524.4 was comparable to that with a conventional ESI source (within 1 order of magnitude). We quantitatively assessed the SAWN−APCI approach from 1−20 $\mu$g/mL in Figure S6 and observe excellent signal down to the lowest concentration studied (1 $\mu$g/mL).

When the same solution was analyzed with an ESI source, only $[M + 2H]^{2+}$ was detected without $MH^+$. Such evidence suggests that alternative mechanisms for droplet ionization and desolvation may be at play, distinct from ESI. Following this, two synthetic peptides were investigated for their charge-state distributions and enhancement effects. Their structures can be found in Figure S-1.

A synthetic peptide featuring two basic lysines ($C_{35}H_{62}N_6O_4$, monoisotopic mass of 630.5 g mol$^{-1}$, termed Peptide-1) was tested with SAWN and SAWN−APCI approaches. The resulting mass spectrum obtained with SAWN (cf. Figure 6a) showed singly and doubly charged

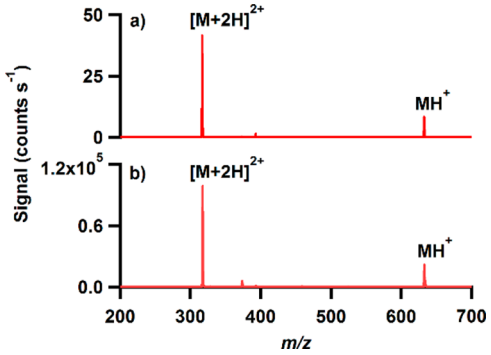


**Figure 6.** Mass spectra of Peptide-1 $C_{35}H_{62}N_6O_4$ (monoisotopic mass 630.5), (a) with APCI off and (b) with APCI on.

analyte ions. Specifically, the singly charged analyte ion was 25% of the doubly charged. With APCI activation, ion signals of both $MH^+$ and $[M + 2H]^{2+}$ increased by almost 4 orders of magnitude (cf. Figure 6b) without changing the charge-state distribution.

A higher mass peptide ($C_{56}H_{95}N_9O_6$, monoisotopic mass of 989.7 g mol$^{-1}$, termed Peptide-2) incorporating three lysines, was also tested. Similarly, the ion signals of $[M + 2H]^{2+}$ and $MH^+$ corresponding to Peptide-2 increased by 3 orders of magnitude (cf. Figure 7), when the APCI was activated. In this case, the singly protonated ion is 10% of the doubly protonated. Notably, with the third lysine as a site for protonation, little $[M + 3H]^{3+}$ is observed in the lower mass range (Figure S7).

**Proposed Mechanism of SAWN−APCI Enhancement.** The performance of SAWN as a sample introduction mechanism strongly depends on further investigation into its nebulization behavior. Thus, to further elucidate the mechanism of the enhanced ionization efficiency observed in this study, we theoretically calculated the mean particle diameter produced by the SAWN device used in our present


DOI: 10.1021/acs.analchem.8b03927
Anal. Chem. 2019, 91, 912−918

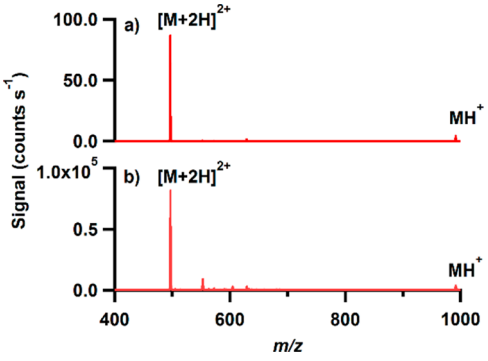


**Figure 7.** Mass spectra of Peptide-2 $C_{55}H_{95}N_9O_6$ (monoisotopic mass = 989.7 g mol$^{-1}$) with APCI (a) off and (b) on.

work. The caffeine being dissolved in a methanol/water mixture of 50:50 volumetric ratio, the surface tension of the mixture was calculated with[39]

$$\sigma = y_a\sigma_a + y_b\sigma_b \quad (1)$$

where $y_a$ and $y_b$ are the fractions of components a and b, respectively, and $\sigma_a$ and $\sigma_b$ are the surface tensions of the pure component solvents. Note that the changes in surface tension induced by dissolving caffeine were neglected to simplify the calculation. The mean particle diameter was then calculated according to the laboratory temperature, i.e., 25 °C, with[40]

$$d_{mean} = \kappa\cdot\lambda = \kappa\cdot\left(\frac{8\pi\sigma}{\rho f^2}\right)^{1/3} \quad (2)$$

where $d_{mean}$ is the mean particle/aerosol diameter, $\kappa$ is an empirically noted proportionality constant of 0.34,[41] $\sigma$ is the surface tension of the bulk solution, $\rho$ is the density, where 0.787 g/mL was used,[42] and $f$ is the frequency of the SAW, which is 9.56 MHz.[40] The mean particle diameter was determined to be ca. 300 nm. As noted by Lang, the initial particle size distribution of ultrasonically generated particles is not considered monodisperse, and the vast majority (>90%) exhibit particle sizes less than *twice* the calculated, theoretical mean diameter.[41] For a nominally similar ultrasonic nebulizer operating at 9.6 MHz, Kurosawa estimates that less than 5 in every 1000 solvent molecules is efficiently converted into the particulate phase.[40] This phenomenon may be explained by the Kelvin curvature effect,[43] which relates higher vapor pressures with diminishing particle size and is particularly relevant to sub-micrometer particles.[44] By extension, the estimated majority of the small particles that we generate spans a critical border between favorable evaporation conditions and favorable coagulation/growth conditions. We then infer that, through efficient solvent evaporation, we observe very effective desorption of our neutral analytes through SAWN.

Nonetheless, particles of these sizes may still contain a significant number of molecules of analyte and solvent. With the presence of a strong electric field induced by the APCI needle, electrospray may occur on individual droplets during its transportation toward the inlet of the mass spectrometer. This phenomenon has been reported as in-flight electrospray.[45] Verifying that the corona discharge at the APCI needle is key to ion-signal enhancement, the APCI source was modified. Instead of the conventional needle tip, a round tungsten bar ($\Phi$ = 2 mm) with a polished spherical tip was used to avoid the formation of corona discharge.[46] If in-flight electrospray on the microdroplets is the mechanism of ion-signal enhancement, the removal of the corona discharge should not affect the enhancement. In fact, no enhancement was observed without the presence of the corona plasma. In addition, the number of charged droplets that were formed during the rapid atomization[22,23,47] was negligible compared to those induced by APCI. Thus, the enhancement of ionization can only be the result of the corona discharge and/or the reagent ions.

To further deduce the mechanism of enhanced ionization, we prevented direct exposure of the analyte-containing aerosols to the corona discharge by isolating the APCI plasma in a concealed chamber (cf. Figure S2). The corona discharge was established in an ionization source similar to the geometry of a DART and FAPA, where a pin anode and a ring cathode were used.[48] Instead of using conventional helium as the discharge gas, we used nitrogen to sustain a corona plasma and guide the reagent ion species to exit the chamber. Unlike helium, which possesses a much lower density relative to air, the stream of nitrogen minimized the aerodynamic perturbation when the aerosols contact the reagent ions.[49] To produce a comparable and steady reagent ion signal, the concealed source was operated in current-controlled mode with a discharge current of 7 $\mu$A at ca. 3 kV. To minimize the distortion from the ion plume generated by SAWN via the gas stream at the exit of the ionization source, a hole of $\Phi$ = 6.00 mm was drilled and reamed to achieve a flow rate of 0.5 L/min. In contrast to a DART or FAPA source, the gas velocity of this source is ~3 × 10$^{-4}$ m s$^{-1}$, whereas other sources are ~3 m s$^{-1}$.[8,48] The combination of the concealed ionization source with SAWN resulted in signal enhancements of the protonated ion ($MH^+$, $m/z$ 195.1) of caffeine by 9.8 × 10$^1$. Compared to the APCI with an exposed needle that provided 1.4 × 10$^3$ signal increment, this concealed APCI exhibited less ionization enhancement. This reduction may be related to the change of the geometry of the setup. Specifically, the SAWN chip was placed further upstream of the MS inlet because of the size of the concealed ionization source. Even so, our observations support the idea that the reagent ions comprise the most significant source of signal enhancement for small molecules like caffeine.

**Production of Doubly Charged Ions.** The proton and charge-transfer regimes from an ADI source do not lead to the formation of multiply charged species because of Coulomb's force.[50] In fact, ionization through reagent ions then requires multiple consecutive processes of charge/proton transfer. Yet, the doubly charged species dominates the spectrum, while APCI was activated as seen in Figures 5, 6, and 7. Thus, in addition to the reagent ion species that can improve the charging efficiency, the corona discharge also provides an additional ionization mechanism. In contrast, the use of APCI after an ESI source usually reduces the charges from the ionic species.[51] However, the mostly neutral, fine droplets generated by the SAWN may behave differently than those that are charged.

Further investigations with Peptide-1 and Peptide-2 implied a dependency of the charge-state distribution upon the type of analyte. The ratio between singly to doubly charge ions changes from 25to 10% while incorporating an additional lysine (as a site for protonation) in the peptide backbone between Peptide-1 and Peptide-2. Meanwhile, Peptide-1 with two lysines resulted in a mass spectrum highly similar to an ESI source. Both mass spectra exhibited singly charged ion signal at 25% of the doubly charged. In contrast, the ESI mass spectrum


DOI: 10.1021/acs.analchem.8b03927
Anal. Chem. 2019, 91, 912−918

of Peptide-2 (cf. Figure S8) with three lysines exhibits singly charged ion signal at 2.7% of the doubly charged, which is notably smaller than the 10% observed with SAWN−APCI. We speculate that the charge residue mechanism is responsible for the doubly charged species.[52] The fine droplet produced by SAWN enters the APCI discharge region, acquiring multiple charges because of its size while sustained in the corona plasma. During the desolvation, leftover charges bond to the binding site of the peptides similar to ESI processes. Unlike the Taylor cone region during electrospray, where the Rayleigh limit allows more charges per droplet,[53] the interaction between the fine droplets and the corona plasma may be largely constrained by Coulomb's law. Experimentally, this difference can be appreciated by the observation of the triply protonated Peptide-2 in a conventional ESI source (cf. Figure S8), while arguably, no triply charged ions were detected with SAWN−APCI (cf. Figure S7).

## CONCLUSION

The SAWN−APCI method generally proved to enhance ionization efficiency over SAWN alone for the analytes studied in the present work. The method also appeared to expand the applicable range of APCI toward large molecules, which can further enable simple and quick analysis of biomolecule-containing samples with high throughput. Both APCI and SAWN, each known as soft ionization approaches in themselves, retain this gentle behavior when combined. Similar to ESI, we also observed intact molecular ions as well as some with multiple charges. However, the mass spectra acquired through the SAWN−APCI approach is not fully comparable with that of an ESI. Despite the polarities of the analytes studied, signal enhancements were observed through activating the APCI when it is coupled to SAWN. Thus, this method inherits the advantage of APCI in terms of analyzing samples independent of their polarity. Therefore, applications may include hydrocarbon and polymer analyses, for which ESI may not be amenable. Further investigations of different analytes, such as large nonpolar molecules, will be included in future works.

The nature of the enhancement may be the result of leveraging effective means to both desorption and ionization as distinct processes. Neutrals efficiently brought into the gas phase by SAWN are also efficiently ionized by APCI. For SAWN desorption, the production of numerous sub-micrometer particles likely promotes evaporation due to the Kelvin curvature effect. Meanwhile, our investigations toward the mechanism of APCI enhancement suggested that both the discharge itself and the reagent ions enhanced the ion signal simultaneously. In particular, the corona discharge region might be where multiple charging occurs. Future studies regarding the charge-state distribution from SAWN−APCI relying upon molecular structure (e.g., proton-binding sites) may reveal the thermal dynamic and kinetic natures of gas-phase ion−molecule/droplet interaction.

## ASSOCIATED CONTENT

### Supporting Information

The Supporting Information is available free of charge on the ACS Publications website at DOI: 10.1021/acs.analchem.8b03927.

Figures S1: Chemical structure of Peptide-2 and Peptide-1; Figure S2: Image of concealed SAWN−APCI setup; Figure S3: Extracted ion chronogram of protonated caffeine at $m/z$ 195.1 without smoothing; Figure S4: Caffeine mass spectra obtained with an ESI source; Figure S5: Comparison between perylene mass spectra; Figure S6: Calibration curve for the analysis of Angiotensin II with the ion peak at $m/z$ 524.42 in the range of 1 to 20 ppm; Figure S7: Confirmation of triply charged Peptide-2; Figure S8: Peptide-2 mass spectra obtained with an ESI source (PDF)

## AUTHOR INFORMATION

### Corresponding Author

*Mailing Address: Theresa Evans-Nguyen, CHE205, 4202 East Fowler Ave, Tampa, FL 33620, United States; Tel.: 813-974-9633; E-mail: evansnguyen@usf.edu.

### ORCID

Theresa Evans-Nguyen: 0000-0001-7675-1060

### Notes

The authors declare no competing financial interest.

## ACKNOWLEDGMENTS

We thank Professor Jianfeng Cai at the University of South Florida for the donation of the synthetic peptides. We also thank Dr. Erik Nilsson for guidance in the use of the Deurion SAWN device.

## REFERENCES

(1) Cooks, R. G.; Ouyang, Z.; Takats, Z.; Wiseman, J. M. *Science* **2006**, *311* (5767), 1566−1570.
(2) Monge, M. E.; Harris, G. A.; Dwivedi, P.; Fernández, F. M. *Chem. Rev.* **2013**, *113* (4), 2269−2308.
(3) Takats, Z.; Wiseman, J. M.; Gologan, B.; Cooks, R. G. *Science* **2004**, *306* (5695), 471−473.
(4) Chernetsova, E. S.; Morlock, G. E.; Revelsky, I. A. *Russ. Chem. Rev.* **2011**, *80* (3), 235.
(5) Ifa, D. R.; Wu, C.; Ouyang, Z.; Cooks, R. G. *Analyst* **2010**, *135* (4), 669−681.
(6) Gross, J. H. *Anal. Bioanal. Chem.* **2014**, *406* (1), 63−80.
(7) Shelley, J. T.; Chan, G. C.-Y.; Hieftje, G. M. *J. Am. Soc. Mass Spectrom.* **2012**, *23* (2), 407−417.
(8) Cody, R. B.; Laramée, J. A.; Durst, H. D. *Anal. Chem.* **2005**, *77* (8), 2297−2302.
(9) Chernetsova, E. S.; Morlock, G. E. *Int. J. Mass Spectrom.* **2012**, *314*, 22−32.
(10) Schaper, J. N.; Pfeuffer, K. P.; Shelley, J. T.; Bings, N. H.; Hieftje, G. M. *Anal. Chem.* **2012**, *84* (21), 9246−9252.
(11) Bierstedt, A.; Riedel, J. *Methods* **2016**, *104*, 3−10.
(12) McEwen, C. N.; Larsen, B. S. *Int. J. Mass Spectrom.* **2015**, *377*, 515−531.
(13) Qi, A.; Friend, J. R.; Yeo, L. Y.; Morton, D. A. V.; McIntosh, M. P.; Spiccia, L. *Lab Chip* **2009**, *9* (15), 2184.
(14) Yeo, L. Y.; Friend, J. R. *Biomicrofluidics* **2009**, *3* (1), 012002.
(15) Heron, S. R.; Wilson, R.; Shaffer, S. A.; Goodlett, D. R.; Cooper, J. M. *Anal. Chem.* **2010**, *82* (10), 3985−3989.
(16) Huang, Y.; Yoon, S. H.; Heron, S. R.; Masselon, C. D.; Edgar, J. S.; Tureček, F.; Goodlett, D. R. *J. Am. Soc. Mass Spectrom.* **2012**, *23* (6), 1062−1070.
(17) Yoon, S. H.; Liang, T.; Schneider, T.; Oyler, B. L.; Chandler, C. E.; Ernst, R. K.; Yen, G. S.; Huang, Y.; Nilsson, E.; Goodlett, D. R. *Rapid Commun. Mass Spectrom.* **2016**, *30* (23), 2555−2560.
(18) Huang, Y.; Heron, S. R.; Clark, A. M.; Edgar, J. S.; Yoon, S. H.; Kilgour, D. P. A.; Turecek, F.; Aliseda, A.; Goodlett, D. R. *J. Mass Spectrom.* **2016**, *51* (6), 424−429.



DOI: 10.1021/acs.analchem.8b03927
*Anal. Chem.* 2019, 91, 912−918

(19) Liang, T.; Schneider, T.; Yoon, S. H.; Oyler, B. L.; Leung, L. M.; Fondrie, W. E.; Yen, G.; Huang, Y.; Ernst, R. K.; Nilsson, E.; et al.etal *Int. J. Mass Spectrom.* **2018**, *427*, 65.
(20) Ho, J.; Tan, M. K.; Go, D. B.; Yeo, L. Y.; Friend, J. R.; Chang, H.-C. *Anal. Chem.* **2011**, *83* (9), 3260−3266.
(21) Dale, S. K.; Lieberman, M.; Go, D. B. Surface Acoustic Wave Nebulization Mass Spectrometry Analysis of Analytes Stored on Paper Substrates. In *Abstracts of Papers of the American Chemical Society*; The American Chemical Society: Washington, DC, **2013**; p 246.
(22) Hirabayashi, A.; Sakairi, M.; Koizumi, H. *Anal. Chem.* **1995**, *67* (17), 2878−2882.
(23) Dodd, E. E. *J. Appl. Phys.* **1953**, *24* (1), 73−80.
(24) Heron, S. R.; Wilson, R.; Shaffer, S. A.; Goodlett, D. R.; Cooper, J. M. *Anal. Chem.* **2010**, *82* (10), 3985−3989.
(25) Yoon, S. H.; Huang, Y.; Edgar, J. S.; Ting, Y. S.; Heron, S. R.; Kao, Y.; Li, Y.; Masselon, C. D.; Ernst, R. K.; Goodlett, D. R. *Anal. Chem.* **2012**, *84* (15), 6530−6537.
(26) Li, J.; Lu, H.; Liu, S.; Xu, Z. *J. Hazard. Mater.* **2008**, *153* (1), 269−275.
(27) Horning, E. C.; Horning, M. G.; Carroll, D. I.; Dzidic, I.; Stillwell, R. N. *Anal. Chem.* **1973**, *45* (6), 936−943.
(28) Blake, R. S.; Monks, P. S.; Ellis, A. M. *Chem. Rev.* **2009**, *109* (3), 861−896.
(29) Shelley, J. T.; Wiley, J. S.; Chan, G. C. Y.; Schilling, G. D.; Ray, S. J.; Hieftje, G. M. *J. Am. Soc. Mass Spectrom.* **2009**, *20* (5), 837−844.
(30) Hunt, D. F.; Crow, F. W. *Anal. Chem.* **1978**, *50* (13), 1781−1784.
(31) Giese, R. W. *J. Chromatogr. A* **2000**, *892* (1), 329−346.
(32) Huang, Y.; Yoon, S. H.; Heron, S. R.; Masselon, C. D.; Edgar, J. S.; Tureček, F.; Goodlett, D. R. *J. Am. Soc. Mass Spectrom.* **2012**, *23* (6), 1062−1070.
(33) Fenn, J. B.; Mann, M.; Meng, C. K.; Wong, S. F.; Whitehouse, C. M. *Science* **1989**, *246* (4926), 64−71.
(34) Yamashita, M.; Fenn, J. B. *J. Phys. Chem.* **1984**, *88* (20), 4451−4459.
(35) Emel'yanenko, V. N.; Verevkin, S. P. *J. Chem. Thermodyn.* **2008**, *40* (12), 1661−1665.
(36) Badal, S. P.; Michalak, S. D.; Chan, G. C.-Y.; You, Y.; Shelley, J. T. *Anal. Chem.* **2016**, *88* (7), 3494−3503.
(37) Cheng, S.-C.; Jhang, S.-S.; Huang, M.-Z.; Shiea, J. *Anal. Chem.* **2015**, *87* (3), 1743−1748.
(38) Coon, J. J.; Harrison, W. W. *Anal. Chem.* **2002**, *74* (21), 5600−5605.
(39) Eberhart, J. G. *J. Phys. Chem.* **1966**, *70* (4), 1183.
(40) Kurosawa, M.; Futami, A.; Higuchi, T. *International Solid State Sensors and Actuators Conference (Transducers '97)* **1997**, *2*, 801−804 vol.2 .
(41) Lang, R. J. *J. Acoust. Soc. Am.* **1962**, *34* (1), 6−8.
(42) Mikhail, S. Z.; Kimel, W. R. *J. Chem. Eng. Data* **1961**, *6* (4), 533−537.
(43) Skinner, L. M.; Sambles, J. R. *J. Aerosol Sci.* **1972**, *3*, 199−210.
(44) Rader, D. J.; McMurry, P. H.; Smith, S. *Aerosol Sci. Technol.* **1987**, *6* (3), 247−260.
(45) Kim, O. V.; Dunn, P. F. *Langmuir* **2010**, *26* (20), 15807−15813.
(46) Sekimoto, K.; Takayama, M. *Eur. Phys. J. D* **2010**, *60* (3), 589−599.
(47) Loeb, L. B. Static Charging by Spray Electrification. *Static Electrification*; Springer-Verlag: Berlin, 1958; pp 58−124.
(48) Shelley, J. T.; Wiley, J. S.; Hieftje, G. M. *Anal. Chem.* **2011**, *83* (14), 5741−5748.
(49) Pfeuffer, K. P.; Schaper, J. N.; Shelley, J. T.; Ray, S. J.; Chan, G. C.-Y.; Bings, N. H.; Hieftje, G. M. *Anal. Chem.* **2013**, *85* (15), 7512−7518.
(50) Schwartz, A. J.; Shelley, J. T.; Walton, C. L.; Williams, K. L.; Hieftje, G. M. *Chem. Sci.* **2016**, *7* (10), 6440−6449.
(51) Ebeling, D. D.; Westphall, M. S.; Scalf, M.; Smith, L. M. *Anal. Chem.* **2000**, *72* (21), 5158−5161.
(52) Fernandez de la Mora, J. *Anal. Chim. Acta* **2000**, *406* (1), 93−104.
(53) *Selected Topics in Mass Spectrometry in the Biomolecular Sciences*; Caprioli, R. M., Malorni, A., Sindona, G., Eds.; Springer Netherlands: Dordrecht, 1997.


DOI: 10.1021/acs.analchem.8b03927
*Anal. Chem.* 2019, 91, 912−918